

Performance Trades Study for Robust Airfoil Shape Optimization

Wu Li and Sharon Padula

MDO Branch, NASA Langley Research Center, Hampton, VA 23681

From time to time, existing aircraft need to be redesigned for new missions with modified operating conditions such as required lift or cruise speed. This research is motivated by the needs of conceptual and preliminary design teams for smooth airfoil shapes that are similar to the baseline design but have improved drag performance over a range of flight conditions. The proposed modified profile optimization method (MPOM) modifies a large number of design variables to search for nonintuitive performance improvements, while avoiding off-design performance degradation. Given a good initial design, the MPOM generates fairly smooth airfoils that are better than the baseline without making drastic shape changes. Moreover, the MPOM allows users to gain valuable information by exploring performance trades over various design conditions. Four simulation cases of airfoil optimization in transonic viscous flow are included to demonstrate the usefulness of the MPOM as a performance trades study tool. Simulation results are obtained by solving fully turbulent Navier-Stokes equations and the corresponding discrete adjoint equations using an unstructured grid computational fluid dynamics code FUN2D.

Nomenclature

| | |
|--|--|
| c | chord length of airfoil |
| c_d | drag coefficient |
| $\frac{\partial c_d}{\partial D}$ | gradient of c_d with respect to D |
| $\frac{\partial c_d}{\partial \alpha}$ | derivative of c_d with respect to α |
| c_l | lift coefficient |
| $\frac{\partial c_l}{\partial D}$ | gradient of c_l with respect to D |
| $\frac{\partial c_l}{\partial \alpha}$ | derivative of c_l with respect to α |
| c_l^* | target lift coefficient |
| D | design vector |
| ΔD | change in design vector |
| $E(\cdot)$ | mean of random variable |
| \mathcal{F} | feasible set for the design vector D |
| M | free-stream Mach number |
| n | number of design variables |
| $p(M)$ | probability density function of Mach number |
| r | number of design conditions |
| x, y | coordinates of points on the plane |
| α | angle of attack |
| γ_k | target drag reduction rate |
| $\delta_{k,i}, \rho_k$ | scalars defining the trust region |
| Ω | a given Mach range |
| $\sigma^2(\cdot)$ | variance of random variable |

Copyright © 2003 by the American Institute of Aeronautics and Astronautics, Inc. No copyright is asserted in the United States under Title 17, U.S. Code. The U.S. Government has a royalty-free license to exercise all rights under the copyright claimed herein for Governmental Purposes. All other rights are reserved by the copyright owner.

| | |
|--------------------------------|----------------------------------|
| $\tau_{k,i}$ | trades factors |
| $\langle \cdot, \cdot \rangle$ | inner product in Euclidean space |

Subscripts and Superscripts

| | |
|-----|--------------------------------------|
| i | index for design condition |
| j | index for component of design vector |
| k | index for iteration or iterate |

Introduction

With tremendous advances in sensitivity calculation by using either continuous or discrete adjoint methods, lift-constrained drag minimization methods or variations (called direct optimization) for aerodynamic shape optimization are gradually gaining acceptance in engineering design community.¹ The most notable one is Boeing's use of TRANSAIR in its commercial aircraft design process. However, inverse design tools^{2,3} are still very popular among designers working on real-world design projects.

Intrigued by Drela's discovery⁴ that multipoint optimization method for lift-constrained drag minimization might produce airfoils with shock bumps corresponding to design conditions, resulting in off-design performance degradation, researchers at NASA Langley Research Center initiated activities to address off-design performance degradation problems by using various robust optimization approaches⁵⁻⁸ with the design space parameterized by B-spline control points. Interestingly, Nemec, Zingg, and Pulliam⁹ used B-spline control points as design variables for multipoint airfoil shape optimization, and obtained an optimal

airfoil that seems to be free of off-design performance degradation (see figure 16 in Ref. 9).

Despite these efforts, a barrier for practical application of lift-constrained drag minimization methods is that a desirable drag rise curve does not necessarily mean a useful airfoil design. Many design aspects can not be captured by optimization models that are based only on lift-constrained drag minimization or its variations.

Our recent effort is to find out whether we can generate realistic airfoil shapes by using a lift-constrained drag minimization approach for design problems. Simulation results given in Ref. 10 indicate that by solving a lift-constrained drag minimization problem adaptively, it is possible to produce fairly realistic improved airfoils with no off-design performance degradation. Encouraged by the preliminary simulation results given in Ref. 10, we wanted to find out whether we could use the profile optimization method proposed by Li et al.⁵ as a performance trades study tool for airfoil shape optimization problems. The result is the modified profile optimization method (MPOM) proposed in this paper. We will use four simulation cases to demonstrate that (i) the MPOM can generate fairly realistic improved airfoil designs in transonic viscous flow, (ii) the trades strategies in MPOM are intuitive to users and easy to use, and (iii) the MPOM allows users to generate an improved airfoil design in each optimization iteration (a benefit of descent optimization methods).

The paper is organized as follows. First, we present the standard robust optimization formulation for airfoil shape optimization, which is the theoretical foundation for the MPOM. Then we give a fairly detailed description of MPOM. Numerical results for four simulation cases of redesigns of the RAE2822 airfoil⁴ and Whitcomb's integral supercritical airfoil¹¹ in transonic viscous flow are included to demonstrate the potential of the MPOM as a practical performance trades study tool. The paper ends with concluding remarks.

Robust Optimization Model for Airfoil Shape Optimization

One plausible approach to avoid off-design performance degradation is to use the standard robust optimization model,¹² which is a multiobjective optimization problem that seeks to minimize both the mean and variance of a performance measure (such as drag). For lift-constrained drag minimization over a range of Mach numbers, a robust optimization problem can be formulated as follows:

$$\min_{D, \alpha(M)} (E(c_d), \sigma(c_d)) \quad (1)$$

subject to $D \in \mathcal{F}$ and

$$c_l(D, \alpha(M), M) = c_l^*(M) \quad \text{for } M \in \Omega. \quad (2)$$

Here $c_l^*(M)$ is the target lift requirement for Mach number M , \mathcal{F} is a given feasible set for geometric design variables (that could be defined by geometry constraints such as specified thickness constraints), and $\alpha(M)$ is the angle of attack corresponding to M . The drag and lift coefficients are c_d and c_l , respectively. The mean and variance of c_d are defined as

$$E(c_d) = \int_{\Omega} c_d(D, \alpha(M), M) \cdot p(M) dM,$$

$$\sigma^2(c_d) = \int_{\Omega} [c_d(D, \alpha(M), M) - E(c_d)]^2 p(M) dM,$$

where $p(M)$ is a probability density function of M and Ω is a given Mach range (such as from $M = 0.68$ to $M = 0.77$). Note that it is important to use equality constraints for the target lift instead of inequality constraints for the minimum lift ($c_l \geq c_l^*$). The latter tends to confuse an optimization code when increasing the angle of attack can increase the lift and reduce the drag simultaneously.

The robust optimization model (1) addresses some important issues in aerodynamic shape optimization. For example, to avoid off-design performance degradation, one can reduce $\sigma(c_d)$ as much as possible. Note that if $\sigma(c_d) = 0$, the corresponding optimal airfoil will have the same (perhaps poor) performance over the given Mach range. On the other extreme, one could minimize $E(c_d)$ as much as possible to improve the average performance. In general, Pareto solutions to (1) can be used to study trade-offs between average performance improvement and performance fluctuations over the Mach range. However, due to the high computational cost for solving Navier-Stokes equations, it is not practical to obtain reasonable estimates of $E(c_d)$ and $\sigma(c_d)$.

One alternative way to avoid off-design performance degradation is to find a descent direction that could reduce the drag *simultaneously* and *proportionally* over the given Mach range while keeping the lift at the target value. The profile optimization method was designed to find such a descent direction with the limited information on lift and drag over the given Mach range. The innovative feature of the profile optimization method is to adaptively change the objective function from iteration to iteration to achieve simultaneous and proportional drag reduction over the given Mach range, which results in an improved design with no off-design performance degradation. In contrast to methods that minimize one aggregate objective function to find a Pareto optimal solution to a multiobjective optimization problem, the profile optimization method does not solve any optimization problem with one predetermined objective function; instead, it looks for a Pareto optimal solution that has the least chance of off-design performance degradation. Using numerical simulations, we demonstrated that the profile optimization method has the potential

to be used by designers for generating practical robust designs.¹⁰

In the next section, we introduce the MPOM that could be used for exploring Pareto optimal solutions of (1).

Modified Profile Optimization Method

Let D^0 be a given initial design vector, let M_1, \dots, M_r be a set of design points over the given Mach range, and $k = 0$. Construct a sequence of design vectors as follows:

1. Compute feasible angles of attack. Find $\alpha_{1,k}, \alpha_{2,k}, \dots, \alpha_{r,k}$ such that

$$c_l(D^k, \alpha_{i,k}, M_i) = c_{l,i}^* \quad \text{for } 1 \leq i \leq r.$$

2. Solve a trust region subproblem. Let $c_{d,i,k}$ and $c_{l,i,k}$ be the linear approximations of the drag and lift at $(D^k, \alpha_{i,k})$:

$$\begin{aligned} c_{l,i,k}(\Delta D, \Delta \alpha_i) &= c_l(D^k, \alpha_{i,k}, M_i) \\ &\quad + \left\langle \frac{\partial c_l}{\partial D}, \Delta D \right\rangle + \frac{\partial c_l}{\partial \alpha} \Delta \alpha_i, \\ c_{d,i,k}(\Delta D, \Delta \alpha_i) &= c_d(D^k, \alpha_{i,k}, M_i) \\ &\quad + \left\langle \frac{\partial c_d}{\partial D}, \Delta D \right\rangle + \frac{\partial c_d}{\partial \alpha} \Delta \alpha_i, \end{aligned}$$

where the derivatives are evaluated at $(D^k, \alpha_{i,k}, M_i)$. Choose a target drag reduction rate γ_k (about 1%–4%) and trade-off factors $\tau_{k,i}$ with $0 < \tau_{k,i} \leq 1$. Consider the following trust region subproblem:

$$\min_{\Delta D, \Delta \alpha_i} \eta \quad (3)$$

subject to

$$\begin{aligned} D^k + \Delta D &\in \mathcal{F}, \\ -\delta_{j,k} \rho_k \leq \Delta D_j &\leq \delta_{j,k} \rho_k \quad \text{for } 1 \leq j \leq n, \\ -\alpha_k \leq \Delta \alpha_i &\leq \alpha_k \quad \text{for } 1 \leq i \leq r, \\ c_{l,i,k}(\Delta D, \Delta \alpha_i) &= c_{l,i}^* \quad \text{for } 1 \leq i \leq r, \\ c_{d,i,k}(\Delta D, \Delta \alpha_i) &\leq (1 - \eta \tau_{k,i}) \cdot c_d(D^k, \alpha_{i,k}, M_i) \\ &\quad \text{for } 1 \leq i \leq r, \end{aligned}$$

where $\delta_{j,k} \geq 0$, $\rho_k > 0$, and $\alpha_k > 0$ are scalars that determine the trust region, and $D^k + \Delta D \in \mathcal{F}$ means that the airfoil corresponding to $(D^k + \Delta D)$ satisfies all the geometric constraints. (For our simulation runs, $\delta_{i,k}$ is approximately the thickness of the airfoil at the x -coordinate of the i th control point, $\alpha_k = 1$ (because feasible angles of attack are determined by the target lift constraints and the shape change), and $D^k + \Delta D \in \mathcal{F}$ means that the airfoil satisfies thickness constraints at two spar locations and at the maximum thickness location.) Determine the smallest

$\rho_k > 0$ such that (3) is feasible and the least norm solution $(\Delta D^k, \Delta \alpha_{1,k}, \dots, \Delta \alpha_{r,k})$ of (3) satisfies the following condition:

$$c_{d,i,k}(\Delta D^k, \Delta \alpha_{i,k}) \leq (1 - \gamma_k \tau_{k,i}) c_d(D^k, \alpha_{i,k}, M_i) \quad \text{for } 1 \leq i \leq r.$$

3. Generate the new iterate. Let $D^{k+1} = D^k + \Delta D^k$.
4. Start a new iteration. Update k by $k + 1$ and go back to step 1.

In the special case when $\tau_{k,i} = 1$, the MPOM reduces to the profile optimization method proposed by Li et al.⁵ The MPOM tries to find a Pareto solution of the following multiobjective optimization problem:

$$\min_{D, \alpha_1, \dots, \alpha_r} (c_d(D, \alpha_1, M_1), \dots, c_d(D, \alpha_r, M_r)) \quad (4)$$

subject to

$$D \in \mathcal{F} \quad \text{and} \quad c_l(D, \alpha_i, M_i) = c_{l,i}^* \quad \text{for } 1 \leq i \leq r.$$

The multipoint optimization method is a weighted sum approach for solving (4). The MPOM is an adaptive minimax approach for solving (4). It can be used interactively by designers to explore various ways to reduce the drag over the given Mach range by using different values of $\tau_{k,i}$.

If γ_k is adjusted according to certain convergence criteria and the multiobjective optimization problem (4) satisfies certain regularity conditions, then it is possible to prove that any accumulation point of the generated iterate sequence is a Pareto optimal solution. Because our focus is to develop practical tools for airfoil shape optimization, we do not address the convergence issue herein.

It is worth pointing out that a simultaneous reduction of the drag over the Mach range always decreases the mean of the drag, while proportional reduction of the drag over the Mach range may decrease the variance of the drag.⁸ Therefore, the MPOM can be considered as an approximation method for finding a Pareto solution to (1) by solving (4) adaptively.

Numerical Simulation Results

We use the MPOM for four cases of airfoil shape design optimization in transonic viscous flow, with target drag reduction rate $\gamma_k = 2\%$ for all the iterations.

The first two cases simulate redesigns of the RAE2822 airfoil¹⁴ over the Mach range from 0.68 to 0.76. We adopt the four design conditions used in Drela's simulation:⁴ $M_1 = 0.68$, $M_2 = 0.71$, $M_3 = 0.74$, and $M_4 = 0.76$, with the target lift at 0.733 and Reynolds number 2.7×10^6 . The first case uses the profile optimization method (i.e., $\tau_{k,i} = 1$), which tries to reduce the drag at all the design conditions simultaneously and proportionally. The second case uses the

modified profile optimization method with the trade-off factors $\tau_{k,i} = 0.1$ for $i = 1, 2, 3$ and $\tau_{k,4} = 1$, which tries to reduce the drag at $M = 0.76$ while keeping the drag at the other design conditions unchanged or improved.

The last two cases simulate redesigns of Whitcomb's integral supercritical airfoil¹¹ over the Mach range from 0.68 to 0.77. For these two cases, we use the following four design conditions: $M_1 = 0.68$, $M_2 = 0.71$, $M_3 = 0.74$, and $M_4 = 0.77$, with the target lift at 0.7 and Reynolds number 2.7×10^6 . For target lift at 0.7, the intended cruise condition for supercritical airfoils (with 11% maximum thickness) is about $M = 0.77$ (see figure 29 in Ref. 11). The third case uses the profile optimization method and the fourth case uses the MPOM with the same trade-off factors as in case 2.

Computational Models

For a given airfoil, the lift and drag coefficients and their gradients are calculated by solving fully turbulent Navier-Stokes equations and the corresponding discrete adjoint equations using an unstructured grid computational fluid dynamics code FUN2D.¹³ In both cases, the unstructured grid has 300 grid points on the airfoil and 32 grid points on the far field (which is placed at 20 chord lengths). The unstructured grid has a total of 18660 grid points, 55649 elements, and 37320 faces, which is almost the same as the grid used in Ref. 10. With the given grid, the flow solver and the adjoint solver are terminated when the 2-norms of the residual of the density equations and its adjoint counterpart are reduced by at least five orders of magnitude.

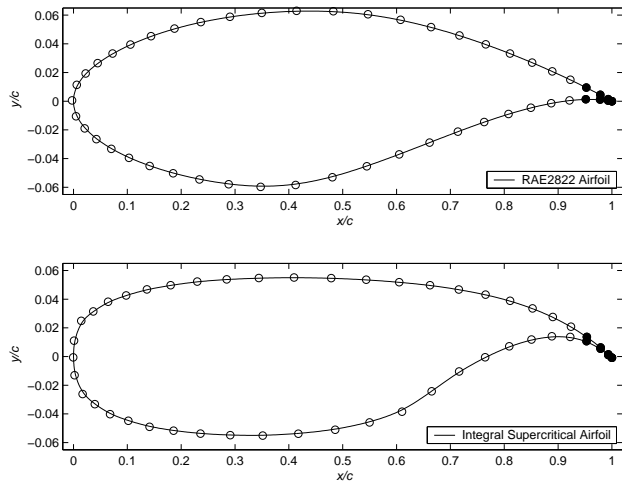


Fig. 1 RAE2822 airfoil and Whitcomb's integral supercritical airfoil parameterized by 51 cubic B-spline control points.

Airfoils are parameterized by cubic B-spline control points. See figure 1 for RAE2822 airfoil and Whitcomb's integral supercritical airfoil parameterization. The x -coordinates of all the control points are fixed during optimization. Changes of the y -coordinates of

the seven control points near the trailing edge (black circles in figure 1) are constrained to be the same. We use these geometric constraints because the optimizer may not be able to make a reasonable modification of the shape of the trailing edge at very fine scales. All the y -coordinates of the 51 control points are used as shape design variables. In all cases, we impose a minimum thickness constraint at spar locations $x/c = 0.15$ and $x/c = 0.6$ and at the maximum thickness location. For each iterate D^k , we find angles of attack $\alpha_{1,k}, \dots, \alpha_{r,k}$ such that $|c_l(D^k, \alpha_{i,k}, M_i) - c_{l,i}^*|/c_{l,i}^* \leq 0.001$.

Drag Reduction Over the Given Mach Range

Figures 2 and 3 show the history of actual drag changes at the design conditions. Note that the predicted drag values at the design conditions do not necessarily match the actual drag values for a new iterate. For example, for several iterations in case 1, at least one of the linear estimations $c_{l,i,k}(\Delta D^k, \Delta \alpha_{i,k})$ and $c_{d,i,k}(\Delta D^k, \Delta \alpha_{i,k})$ of the lift value $c_l(D^{k+1}, \alpha_{i,k} + \Delta \alpha_{i,k}, M_i)$ and the drag value $c_d(D^{k+1}, \alpha_{i,k} + \Delta \alpha_{i,k}, M_i)$, respectively, is not accurate for $M = 0.68$. Possible sources for the estimation errors include: (i) either ΔD^k or $\Delta \alpha_{i,k}$ is too large for linear Taylor approximations to be accurate, (ii) some of the gradient components are not accurate, and (iii) the geometry change ΔD^k is small, but the B-spline curve corresponding to ΔD^k is oscillatory.⁵ By examining the detailed output information from the MPOM, we found that the estimation errors are mainly due to reasons (i) and (iii).

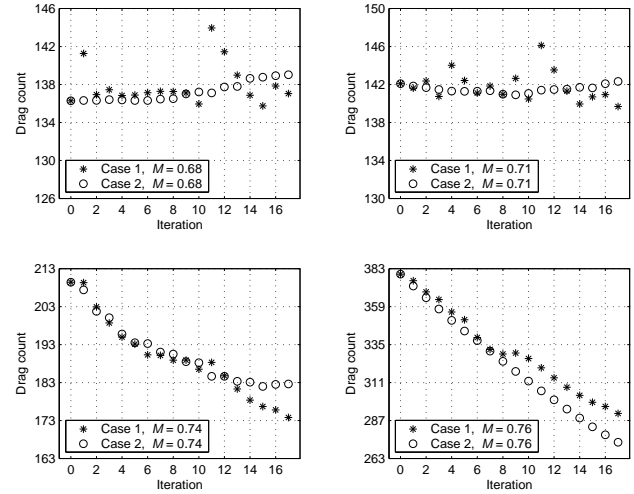


Fig. 2 Changes of drag counts at four design conditions for cases 1 and 2 with target lift 0.733.

For each case, the intended drag reduction strategy will fail after a number of iterations. For example, in case 1, the intended drag reduction at $M = 0.68$ could not be achieved; in case 2, the intent was to reduce the drag at $M = 0.76$ while keeping the drag at other design conditions unchanged or improved. However, at

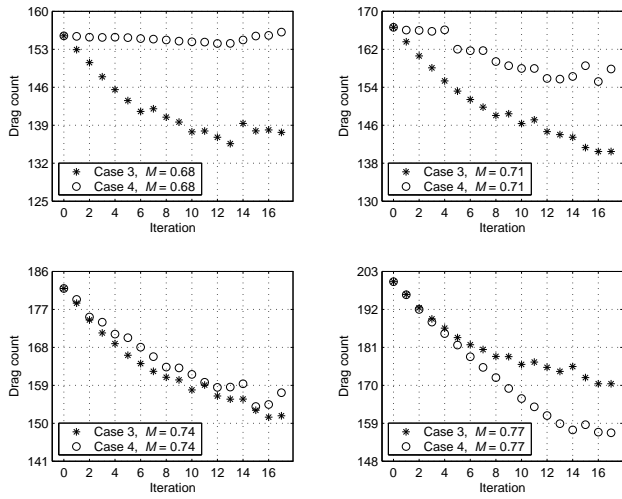


Fig. 3 Changes of drag counts at four design conditions for cases 3 and 4 with target lift 0.7.

the 14th iteration, the drag at the first design condition increases noticeably. In actual design process, perhaps one should increase the values of $\tau_{k,i}$ at $M_1 = 0.68$ and $M_2 = 0.71$ and see whether the MPOM could yield a useful new airfoil according to the intended drag reduction strategy. For comparison purpose, we pick the 10th iterate for cases 1 and 2, while the 13th iterate is selected for cases 3 and 4.

Figure 4 shows the drag rise curves over the Mach range for the selected iterates. The drag rise curves are constructed by using 10 equally spaced Mach numbers from 0.68 to 0.77, which include four design points and six off-design points. The MPOM reduces the drag of the baseline over the given Mach range with no off-design performance degradation, except in case 4 where a drag creep occurs between design points $M = 0.74$ and $M = 0.77$. This is due to excessive drag reduction at $M = 0.77$.

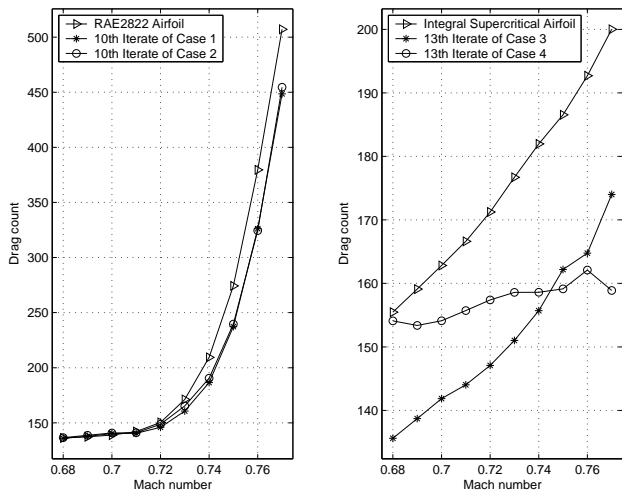


Fig. 4 Postoptimization analysis of drag over the given Mach range. The target lift for cases 1 and 2 is 0.733, while the target lift for cases 3 and 4 is 0.7.

Airfoil Shapes and Pressure Distributions

We include the airfoil shapes and pressure distributions to show that they are quite realistic and that minor modifications of the baseline could lead to significant performance improvement without off-design performance degradation.

Figures 5–8 show the airfoils generated by the MPOM. The vertical lines indicate the locations for thickness constraints. The generated airfoils are not free of bumps. In particular, supercritical airfoils (cases 3 and 4) show bumps at the lower surface near the leading edge and the upper surface near $x/c = 0.7$.

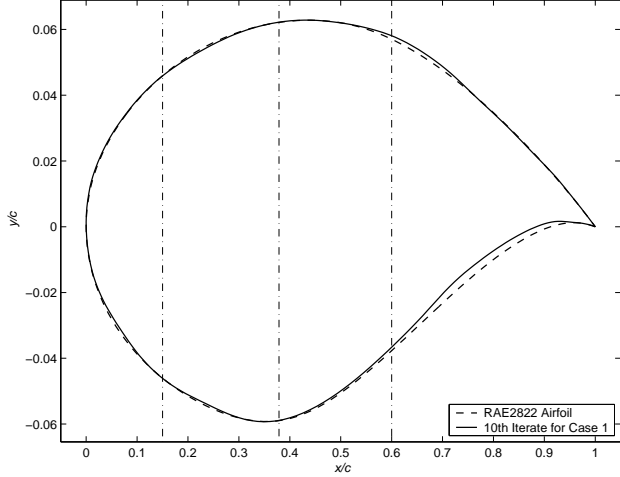


Fig. 5 The 10th airfoil generated by the MPOM for case 1.

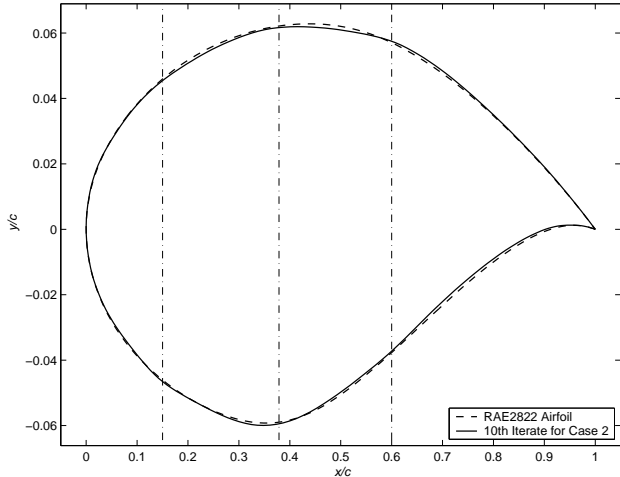


Fig. 6 The 10th airfoil generated by the MPOM for case 2.

Pressure distributions for the baseline and the generated airfoils are plotted in figures 9–12.

Concluding Remarks

From time to time, existing aircraft need to be redesigned for new missions with modified operating conditions such as required lift or cruise speed. This research is motivated by the needs of conceptual and

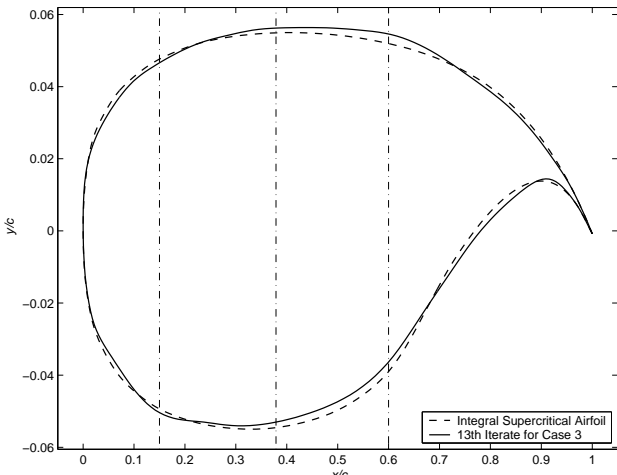


Fig. 7 The 13th airfoil generated by the MPOM for case 3.

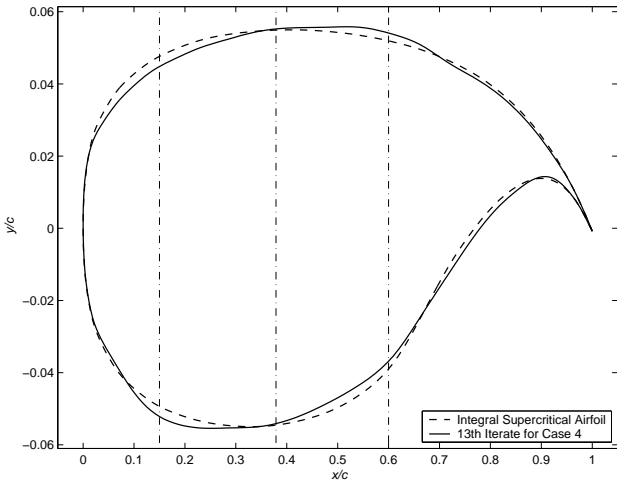


Fig. 8 The 13th airfoil generated by the MPOM for case 4.

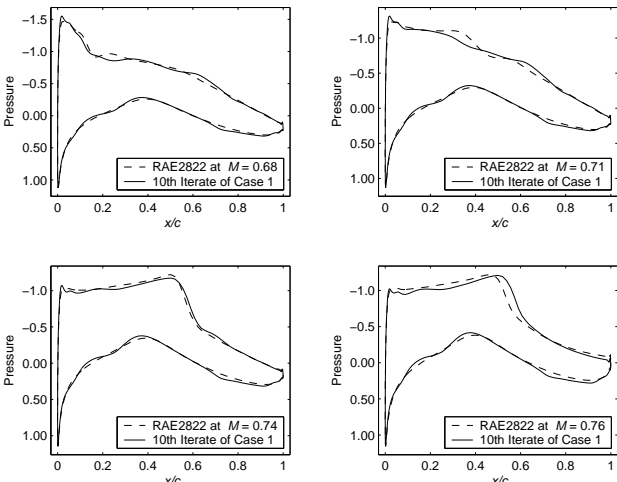


Fig. 9 Pressure distributions at the design conditions for case 1.

preliminary design teams for smooth airfoil shapes that are similar to the baseline design but have im-

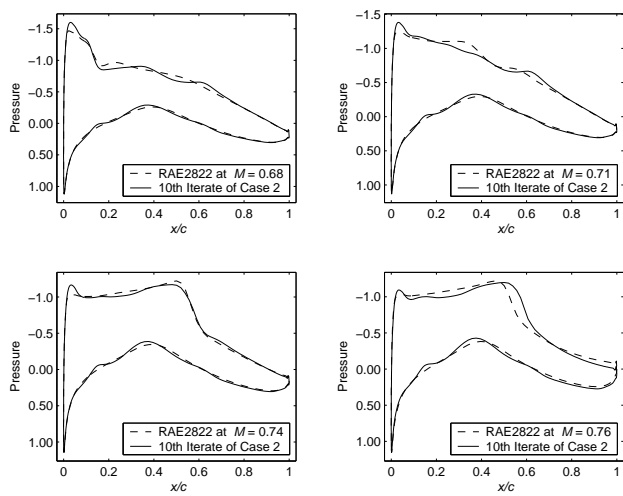


Fig. 10 Pressure distributions at the design conditions for case 2.

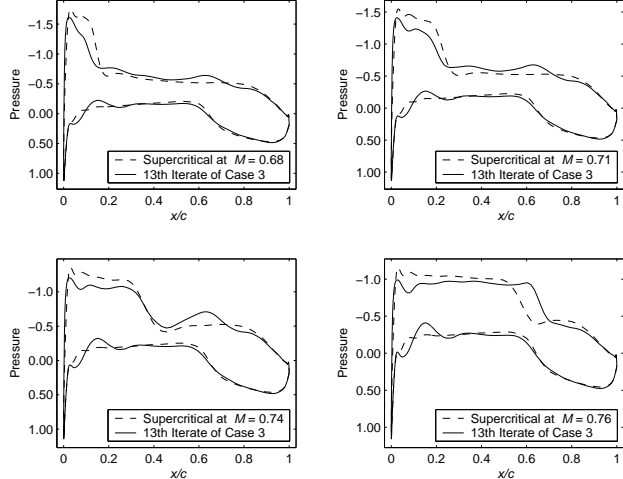


Fig. 11 Pressure distributions at the design conditions for case 3.

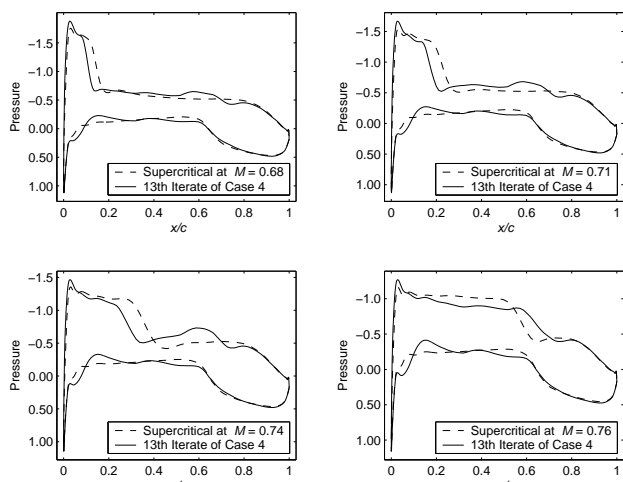


Fig. 12 Pressure distributions at the design conditions for case 4.

proved drag performance over a range of flight conditions. The MPOM modifies a large number of de-

sign variables to search for nonintuitive performance improvements, while avoiding off-design performance degradation. Given a good initial design, the MPOM generates fairly smooth airfoils that are better than the baseline without making drastic shape changes. Moreover, users gain valuable information by exploring performance trades over various design conditions.

The MPOM allows users to choose different rates of drag reduction at the design conditions for performance trades study. The strategy of forcing simultaneous (predicted) drag reduction at all design conditions helps to alleviate off-design performance degradation that weighted average approaches of multipoint optimization methods might encounter when a high resolution design space is used. However, it is important not to reduce drag excessively at a particular design point in order to prevent off-design performance degradation.

We use four cases of airfoil shape optimization in transonic viscous flow to demonstrate the usefulness of the MPOM as a performance trades study tool. An unstructured grid computational fluid dynamics code, FUN2D,¹³ is used to predict the lift and drag values and their gradients with respect to changes in airfoil shape and angle of attack. The MPOM is able to generate fairly smooth airfoils with no off-design performance degradation over the range of Mach numbers with 51 B-spline coefficients as design variables and 4 design conditions.

To use airfoils generated by the MPOM for design projects, postoptimization airfoil smoothing is still necessary. Of course, the performance characteristics of the resulting airfoil after smoothing is somewhat unpredictable. Our future research will integrate airfoil smoothing and the MPOM so that improved smooth airfoils with no off-design performance degradation can be generated for performance trades study.

Acknowledgments

We would like to thank Richard Campbell and Steve Krist for many stimulating discussions on aerodynamic shape design problems that have helped us understand the difference between design and optimization.

References

- ¹A. JAMESON AND J. VASSBERG, Computational fluid dynamics for aerodynamic design: its current and future impact, AIAA Paper 2001-0538, Jan. 2001.
- ²R. CAMPBELL, Efficient viscous design of realistic aircraft configurations, AIAA Paper, AIAA-98-2539.
- ³K. FUJII AND G. DULIKRAVICH (Eds.), *Recent Development of Aerodynamic Design Methodologies – Inverse Design and Optimization*, Vieweg, Braunschweig/Wiesbaden, Germany, 1999.
- ⁴M. DRELA, Pros and cons of airfoil optimization, in “Frontiers of Computational Fluid Dynamics 1998”, edited by D.A. Caughey and M.M. Hafez, World Scientific, 1998.
- ⁵W. LI, L. HUYSE, AND S. PADULA, Robust airfoil optimization to achieve drag reduction over a range of Mach numbers, Structural and Multidisciplinary Optimization, Vol. 24, No. 1, 2002, pp. 38–50.
- ⁶L. HUYSE, M. LEWIS, S. PADULA, AND W. LI, A probabilistic approach to free-form airfoil shape optimization under uncertainty, AIAA Journal, Vol. 40, No. 9, 2002, pp. 1764–1772.
- ⁷S. PADULA AND W. LI, Options for robust airfoil optimization under uncertainty, Ninth AIAA/USAF/NASA/ISSMO Symposium on Multidisciplinary Analysis and Optimization, September 4-6, 2002, also AIAA Paper AIAA-2002-5602.
- ⁸W. LI AND S. PADULA, Using high resolution design spaces for aerodynamic shape optimization under uncertainty, NASA Technical Paper, NASA/TP-2003-11211, 2003.
- ⁹M. NEMEC, D. ZINGG, AND T. PULLIAM, Multi-point and multi-objective aerodynamic shape optimization, AIAA Paper, AIAA-2002-5548.
- ¹⁰W. LI, Profile optimization method for robust airfoil shape optimization in viscous flow, NASA Technical Memorandum, NASA/TM-2003-11787, 2003.
- ¹¹C. HARRIS, NASA supercritical airfoils – A matrix of family-related airfoils, NASA Technical Paper, NASA/TP-1990-2969, March, 1990.
- ¹²W. FOWLKES AND C. CREVELING, *Engineering Methods for Robust Product Design Using Taguchi Methods in Technology and Product Development*, Addison-Wesley, Reading, MA, 1995.
- ¹³E. NIELSEN, *FUN3D/3D: Fully Unstructured Navier-Stokes*. <http://fun3d.larc.nasa.gov> Accessed April. 23, 2003.